Clinical and molecular findings in a family expressing a novel heterozygous variant of the G elongation factor mitochondrial 1 gene

CHANG SU and FANGFANG WANG

Department of Obstetrics and Gynecology, Women's Hospital, Zhejiang University School of Medicine, Hangzhou, Zhejiang 310006, P.R. China

Received March 31, 2020; Accepted July 29, 2020

DOI: 10.3892/etm.2020.9303

Abstract. The identified mutations in the G elongation factor mitochondrial 1 (GFM1) gene have been associated with heterogeneous clinical features of an early-onset mitochondrial disease in only 25 families. The present study reports the case of two siblings with a novel GFM1 variant and their clinical and laboratory presentations, which included progressive hepatic encephalopathy, failure to thrive and persistent lactic acidemia. Both histological changes and diminished expression of the GFM1 protein were observed in the liver and kidney tissues of the index patient. Whole-exome and Sanger sequencing technologies were used to diagnose the index patient with defective GFM1 using amniocentesis at 32 weeks' gestation. Heterozygous mutations in the GFM1 gene were identified in both siblings: A novel mutation, C1576T in exon 13 inherited from their asymptomatic mother, resulting in a premature stop codon at amino acid position 526 and the previously reported G688A mutation on the boundary between exon 5 and intron 5-6, inherited from their asymptomatic father. In conclusion, the present study reports two siblings carrying a novel GFM1 variant with a rare fatal mitochondrial disease.

Introduction

Mitochondria generates ATP via oxidative phosphorylation (OXPHOS) mediated by OXPHOS complexes I, II, III, IV and V, and the dysfunction of the mitochondrial protein synthesis system is involved in OXPHOS deficiency, leading to mitochondrial disease with early-onset and fatal phenotypes (1). Complexes I, III, IV and V all contain ≥1 mitochondrial DNA (mtDNA) encoded subunit, while complex II is encoded completely by nuclear DNA (1). The G elongation factor mitochondrial 1 (GFM1) gene encodes the nuclear-encoded elongation factor G, mitochondrial (EFG1) protein, which is one of the mitochondrial elongation factors that enforces the elongation-dependent movement of mtDNA encoded transfer (t)RNAs through the mitochondrial ribosomes by removing the de-acetylated tRNA and replacing it with the peptidyl-tRNA as a GTPase (2). In 2004, an association was identified between the mutation of the GFM1 gene and the occurrence of early hepatic encephalopathy, a fatal mitochondrial disease, in two siblings with poor prognosis (3). At present, the total number of GFM1 mutations reported in families is 25 (3-13). In the present study, the clinical, laboratory and molecular results in two siblings with heterozygous GFM1 gene defects, one a novel mutation and the other a previously reported mutation (7), are described.

Materials and methods

Patients. A patient with suspected mitochondrial disease and his asymptomatic parents, aged 33 years, were asked to participate in the present study in February 2019. Written informed consent and consent for publication to use their samples and clinical data were obtained from the parents and the present study was formally approved by the Ethics Committee of The Women's Hospital, Zhejiang University School of Medicine, Zhejiang, China.

Whole-exome and Sanger sequencing. The blood and the amniotic fluid samples were collected and stored at -80˚C until further use. Whole-exome sequencing was performed as previously described by Simon *et al* (11). Single nucleotide variants were confirmed using Sanger sequencing, as previously described (14).

Protein structure analysis. The three-dimensional structure of the EFG1 protein was predicted using the Iterative Threading ASSEmbly Refinement computer modeling program (15). An elimination of part of domain IV and the whole of domain V was predicted with the R526 premature stop codon. The multiple sequence alignment between diverse species was performed using the T-Coffee program (16).

Correspondence to: Dr Fangfang Wang, Department of Obstetrics and Gynecology, Women's Hospital, Zhejiang University School of Medicine, 1 Xueshi Road, Hangzhou, Zhejiang 310006, P.R. China
E-mail: drwangfangfang@zju.edu.cn

Key words: mitochondrial disease, G elongation factor mitochondrial 1, mitochondrial elongation factor

Histological analysis. The hematoxylin and eosin staining procedure was performed. In brief, the collected hepatic and renal tissue samples were fixed for 24 h in 4% paraformaldehyde at 4˚C and embedded in paraffin. Following this, samples were sliced into 4-μm thick sections. For hematoxylin and eosin staining, the slides were stained with hematoxylin for 5 min at room temperature (RT), alcohol hydrochloric acid for 1 sec and eosin for 1 sec. The tissue was observed under an optical microscope (Olympus Corporation; magnification, x200). For immunofluorescence, the slides were immunostained with primary EFG1 polyclonal antibodies (1:50; cat. no. 14274-1-AP; Thermo Fisher Scientific, Inc.) overnight at 4˚C and secondary antibodies (1:2,000; cat. no. A-11036; Thermo Fisher Scientific, Inc.) for 1 h at RT. The nucleus was visualized with DAPI staining for 1 min at RT. Images were taken under a fluorescence microscope (Olympus Corporation; magnification, x150).

Reverse transcription-PCR. Total RNA from the collected hepatic and renal tissue samples were isolated using Total RNA Extraction reagent (cat. no. R401; Vazyme Biotech Co., Ltd.). Following quantification and unified concentrations, total RNA was reversed-transcribed into complementary DNA (cDNA) using a reverse transcription kit (cat. no. R212; Vazyme Biotech Co., Ltd.), according to the manufacturer's protocol. The cDNA was amplified using the Green Taq PCR Mix (cat. no. P131; Vazyme Biotech Co., Ltd.). Primers targeting the GFM1 gene used for PCR analysis were as follows: forward, 5'-CAAAAGGTATTGGCAGGTT-3' and reverse, 5'-CAGGGGCAGTAATGGTCT-3'. The thermocycling conditions were performed at 95˚C for 3 min, followed by 25 cycles of 95˚C for 30 sec, 56˚C for 30 sec and 72˚C for 60 sec.

Western blot analysis. Western blot analysis was performed using whole cell lysates from the liver and kidney of the index patient, as previously described (11), using the following specific antibodies: Anti-NADH:Ubiquinone oxidoreductase subunit A13 (NDUFA13; cat. no. 10986-1-AP; ProteinTech Group, Inc.), anti-succinate dehydrogenase complex iron sulfur subunit B (SDHB; cat. no. ab178423; Abcam), anti-ubiquinol-cytochrome c reductase core protein 2 (UQCRC2; cat. no. ab203832; Abcam), anti-ATP synthase peripheral stalk subunit F6 (ATP5; cat. no. ab176569; Abcam) and anti-GAPDH (cat. no. ab181602; Abcam). Differences in proteins levels were determined by visual inspection.

Results

Clinical features and laboratory findings. At 32 weeks' gestation, the index patient was genetically diagnosed with a defect in the GFM1 gene using amniocentesis. He was born to unrelated Chinese parents, with a pregnancy complicated by a late 3rd trimester suspicion of fetal growth restriction. The vaginal birth, following a previous cesarean section, occurred at 40 weeks' gestation, without any complications and no neonatal resuscitation was required. His birthweight was 2.3 kg and he presented with an omphalocele and an inguinal hernia. Soon after birth, he was admitted to the neonatal unit of Women's Hospital, Zhejiang University School of Medicine and received symptomatic treatment for metabolic acidosis, hypoglycemia, kaliopenia, hypocalcemia, hypernatremia, hepatic impairment and anemia. He was treated with ursodeoxycholic, levocarnitine, vitamins B1, -2, -6 and -12, coenzyme Q10 and mecobalamine. He exhibited failure to thrive with poor weight gain and his body weight was 2.9 kg at 2 months old. From 2 months of age, he developed sporadic twitching in the corners of the mouth and eye blinking; however, there was no noticeable dysmorphic features (Fig. 1A). An electroencephalography identified multifocal epileptiform discharges over the frontal and temporal lobes bilaterally; however, he did not exhibit significant epileptic seizures. His brain magnetic resonance imaging scan indicated symmetric swelling in the frontal and temporal lobes, bilateral centra semiovalia, gyri and white matter (Fig. 1B-F). At 3 months of age, he developed severe metabolic acidosis [pH, 6.979 (normal range 7.350-7.450)]; PCO_2, 11.9 mmHg (normal range, 35.0-48.0 mmHg); PO_2, 164 mmHg (normal range, 83.0-108.0 mmHg); base excess -28.5 mM (normal range, -3.0-3.0 mM); and lactic acid, 22.0 mM (normal range, 0.5-1.6 mM). In the following days, several episodes of acute metabolic acidosis were corrected by intravenous administration of bicarbonate. Furthermore, he had severe liver impairment [albumin 28.5 g/l (normal range, 32.0-52.0 g/l)]; total bile acids, 271 μM (normal range, 0.0-12.0 μM); alanine aminotransferase, 220 U/l (normal range, <50 U/l); aspartate amino transferase, 186 U/l (normal range, 15-60 U/l) and high serum ammonia, 112 mM (normal range, 9-30 mM). However, the levels of blood urea nitrogen and creatinine were not increased. In addition, a blood transfusion was administered due to coagulation abnormalities: Prothrombin time, 49.8 sec (normal range, 9.0-14.0 sec); activated partial thromboplastin time, 110 sec (normal range, 23-38 sec); international normalized ratio, 4.15 (normal range, 0.8-1.2); fibrinogen, 0.21 g/l (normal range, 1.8-4.0 g/l) and anemia [hemoglobin 85 g/l (normal range, 110-155 g/l)]. Unfortunately, he succumbed 4 days later due to multiple organ failure.

The female older sibling of the index patient was born at 39 weeks' gestation by cesarean section due to fetal distress. Her birth weight was 2.2 kg and no neonatal resuscitation was required. After birth, she developed inconsolable crying and opisthotonos posturing. At 2 days old, she received symptomatic treatment in the neonatal unit of the hospital due to lethargy, feeding difficulties and hypoglycemia; however, she did not receive a precise diagnosis. Unfortunately, she succumbed 4 days later.

Postmortem histological analysis. Postmortem histopathology of the index patient revealed irregular hepatic plates, steatosis and cholestasis in the liver (Fig. 2A) and glomerular and tubular necrosis in the kidney (Fig. 2C); however, there was no cardiomyopathy (data not shown). Furthermore, immunofluorescent staining with an EFG1 antibody demonstrated markedly decreased protein expression levels of the GFM1 gene in both the liver and renal tissues from the index patient compared with the control (Fig. 3A-D).

Mutation identification and protein prediction. The whole-exome sequencing and following variant validation using Sanger sequencing, in both the amniotic fluid of the

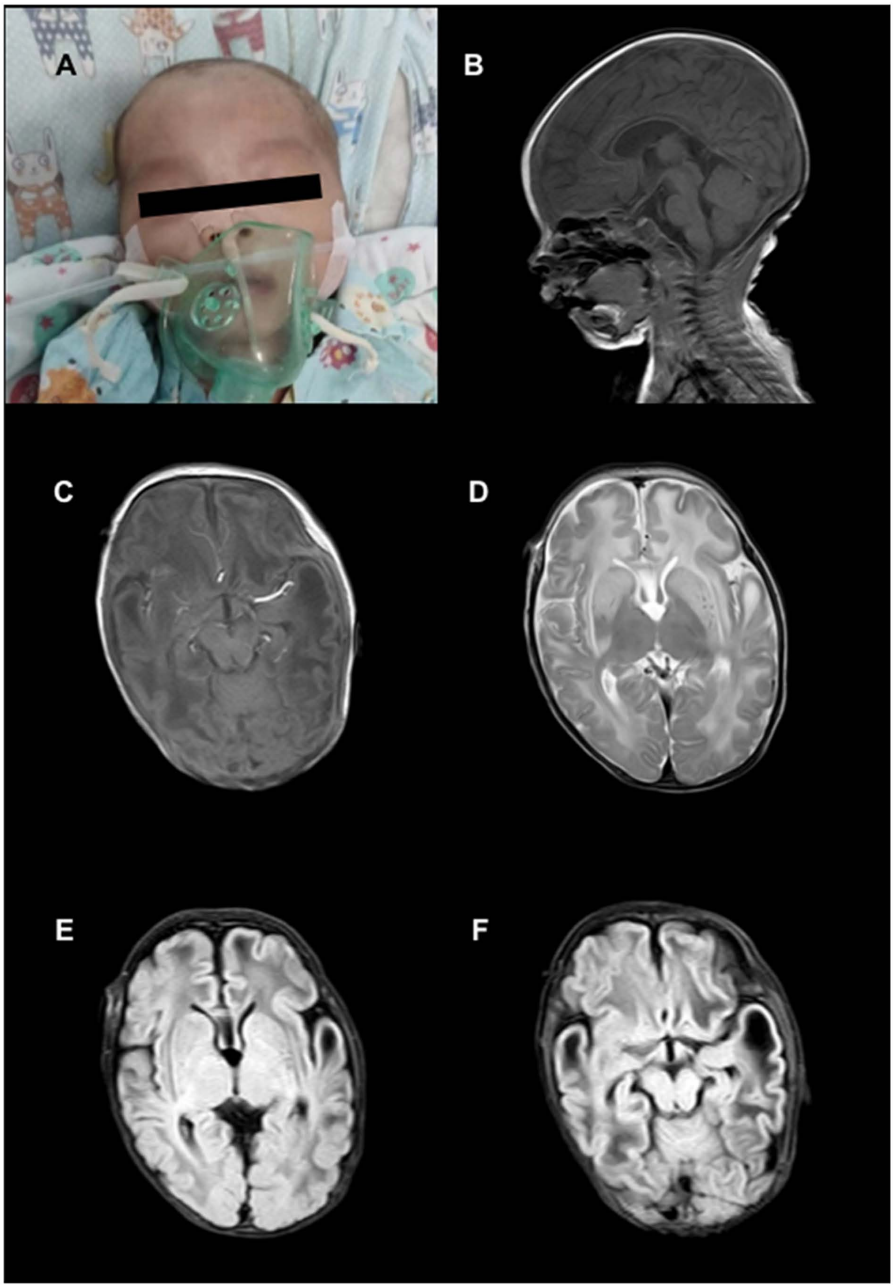

Figure 1. Brain magnetic resonance imaging of the index patient. (A) Image of the 2.5-month-old patient with a normal facial appearance. (B) Midsagittal and (C) axial T1-weighted images, revealed the hypointense symmetric lesions in the frontal and temporal lobes. (D) T2-weighted coronal section exhibited hyperintense symmetric lesions in the frontal and temporal lobes, centra semiovalia, gyri and white matter, and the putamen and globus pallidus. (E and F) T2-fluid attenuated inversion recovery images showing abnormal signals corresponding to those shown in D.

index patient and the blood of his female older sibling, demonstrated that these two patients carried 2 heterozygous mutations in the GFM1 gene (NM_001308166.1): A G688A mutation in the boundary between exon 5 and intron 5-6 (Fig. 4A and B), predicting a glycine to serine substitution at position 230 (Fig. 4C); and a C1576T mutation in exon 13 (Fig. 4A and B), which resulted in a premature stop codon at amino acid position 526 (Fig. 4C). These 2 aforementioned positions have been completely conserved across multiple species (Fig. 4E). Molecular modeling indicated that the G230S substitution changed the secondary and spatial structures in the α-helices and β-sheets of the GTP-binding domain I and the R526 premature stop codon resulted in the loss of the domains IV and V (Fig. 4D) in the EFG1 protein. To understand the origin of the mutations in these patients, genome-wide DNA sequencing from the peripheral blood of both their parents was performed. The results identified that the father was heterozygous for the G688A mutation and wild-type for the C1576T mutation, while the mother was heterozygous for the C1576T mutation and wild-type for the G688A mutation (Fig. 4F).

Effects of the C1576T mutation on GFM1 mRNA variants of the index patient. To examine if the mutant transcript was still present, reverse transcription-PCR followed by sequencing was performed in liver and kidney tissues, and the results

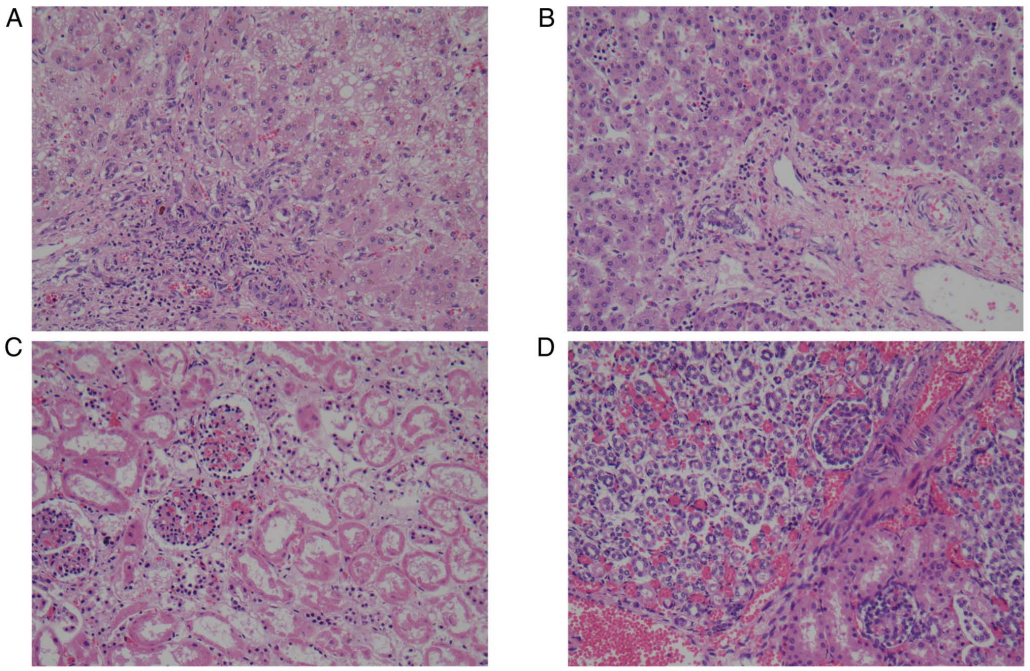

Figure 2. Hematoxylin and eosin histology. Liver tissue exhibited (A) microvesicular steatosis and patchy macrovesicular steatosis, irregular hepatic plates, intrahepatic bile duct hyperplasia, as well as intrahepatic and intracanicular cholestasis, compared with that in the (B) control. (C) Renal tissue exhibiting glomerular and tubular necrosis, compared with that in (D) the control. Magnification, x200.

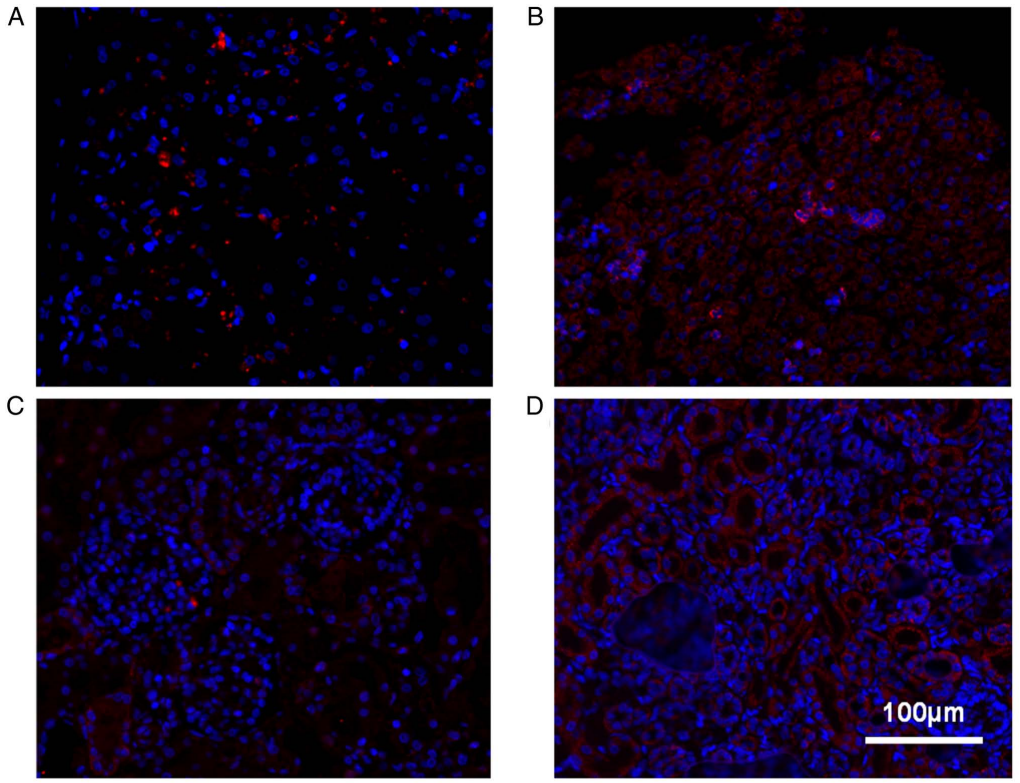

Figure 3. Representative images of indirect immunofluorescence staining for EFG1 in the liver and kidney tissues from the index patient and the control. The expression and location of the EFG1 protein (red) liver tissue from the (A) index patient and (B) the control. The expression and location of the EFG1 protein (red) renal tissue from the (C) index patient and (D) the control. The nucleus was labeled with DAPI (blue). No immunofluorescence staining was detected in the negative control (data not shown). EFG1, elongation factor G, mitochondrial. Scale bar, 100 μm.

identified that the index patient carried the wild-type and mutant GFM1 mRNA variants associated with the c.1576C>T change in a heterozygous manner (Fig. 5A).

Effects of the GFM1 mutations on protein expression in the OXPHOS complex of the index patient. To investigate the subsequent effects of the heterozygous GFM1 mutations on

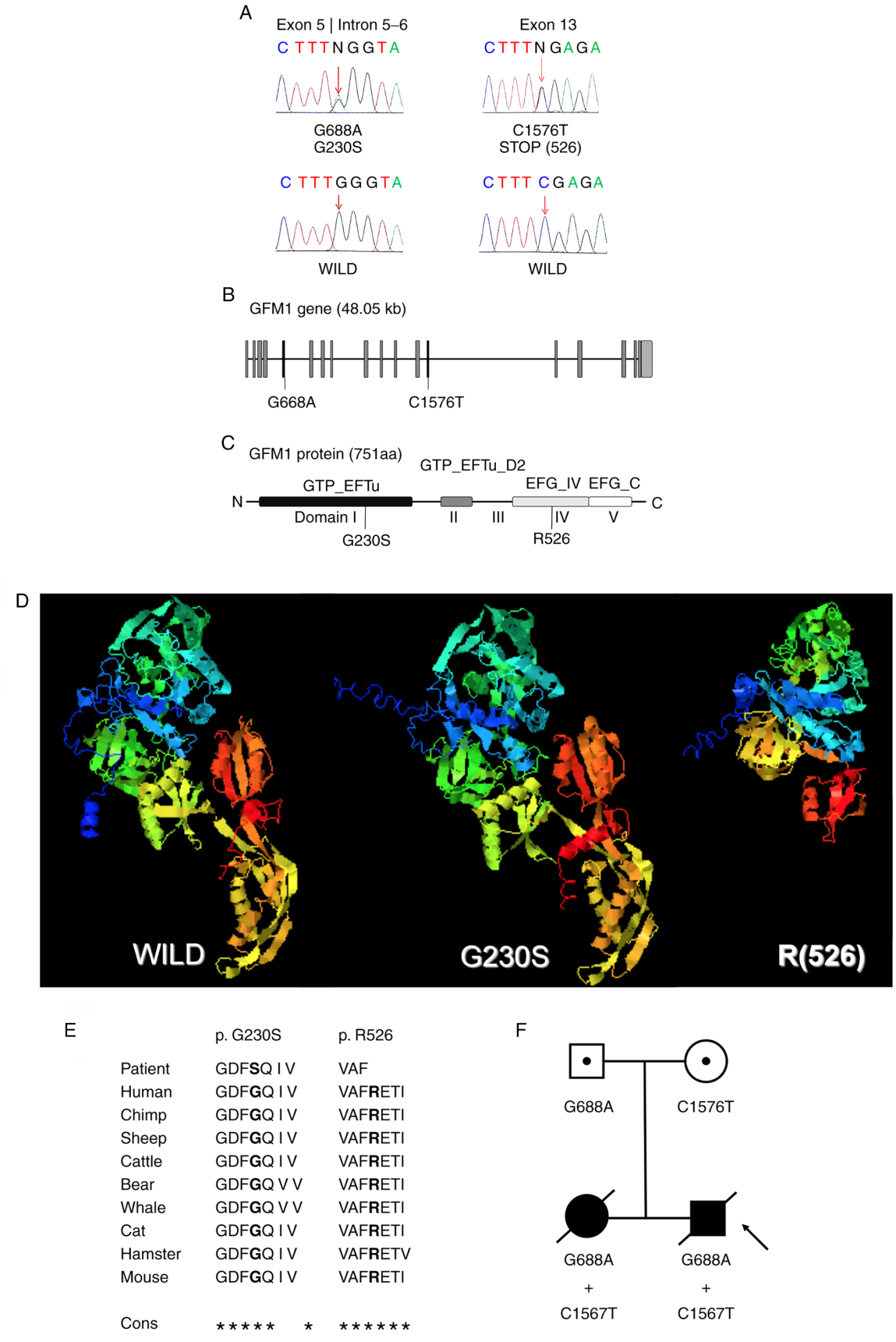

Figure 4. Mutational analysis and protein prediction of GFM1. (A) Sequence analysis of the 2 pathogenic mutations identified in both patients, 1 and 2. The mutations shown are on the sense strand. (B) Schematic representation of the GFM1 gene structure consisting of 18 exons (boxes). The positions of the 2 mutations identified in both patients are shown and the affected exons are represented by the black boxes. (C) The EFG1 protein structure with the corresponding functional domains and the amino acid substitutions predicted by the mutations. The first described GFM1 mutation and substitution are shown with bold fonts. (D) Optimal predicted three-dimensional model of the EFG1 protein structures with the mutations. (E) EFG1 sequence alignment between different species. All the affected amino acids are located in highly conserved regions (marked with an asterisk) across species. (F) Pedigree of the 2 mutations identified in both patients. EFG1, elongation factor G, mitochondrial; GFM1, G elongation factor mitochondrial 1.

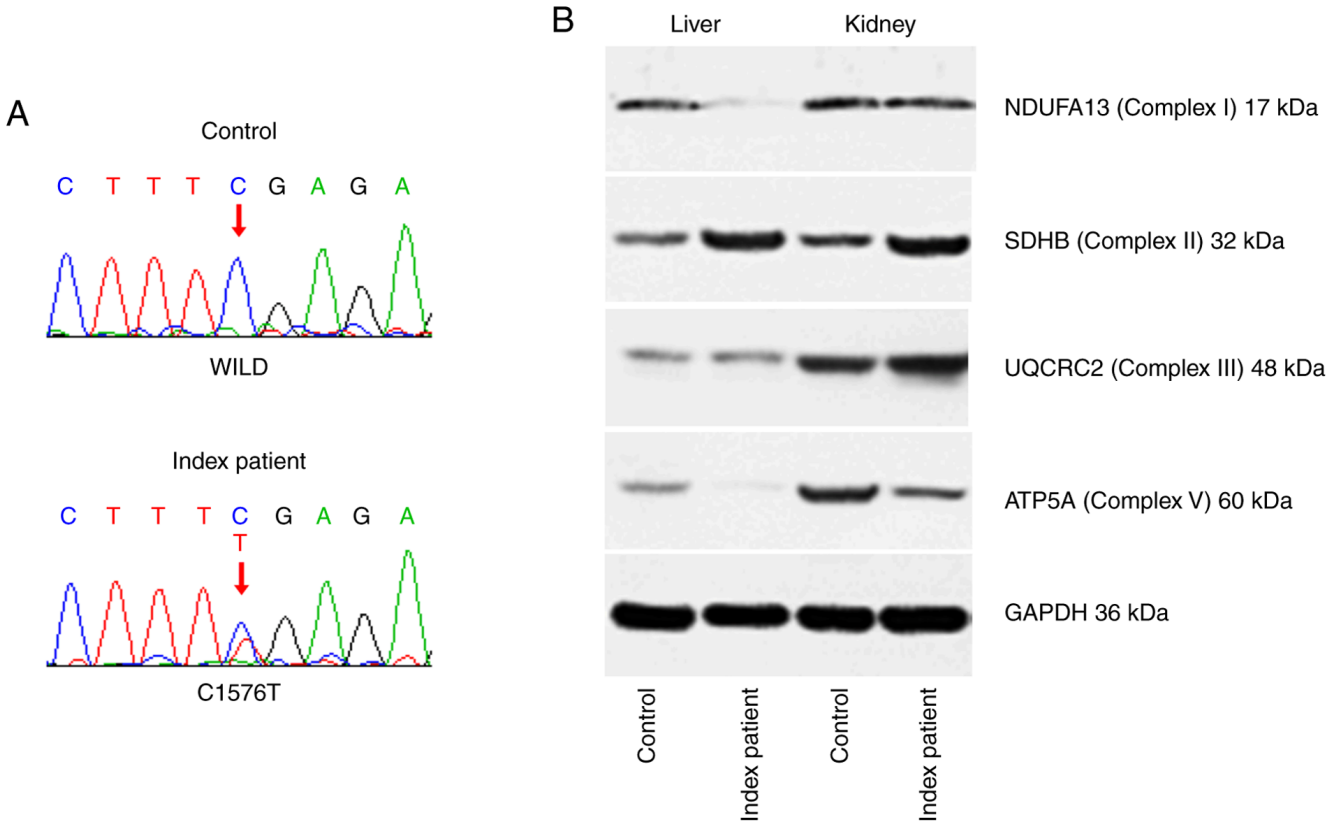

Figure 5. Effects of the GFM1 mutations on mRNA variants and oxidative phosphorylation complex protein expression levels in the liver and kidney tissues from the index patient. (A) The representative results of Sanger sequencing using reverse transcription PCR amplification products showing GFM1 mRNA variants in the liver and kidney tissues of the control and the index patient. (B) Western blot analysis of whole cell extracts from the liver and kidney tissues from the index patient and the control. In the index patient, decreased levels of NDUFA13 and ATP5A were observed in the liver and decreased expression of ATP5A was identified in the kidney. SDHB and GAPDH were used as loading controls. GFM1, G elongation factor mitochondrial 1; NDUFA13, NADH: ubiquinone oxidoreductase subunit A13; SDHB, succinate dehydrogenase complex iron sulfur subunit B; UQCRC2, ubiquinol-cytochrome c reductase core protein 2; ATP5A, ATP synthase peripheral stalk subunit F6.

the expression level changes in representative proteins from the various OXPHOS complexes, western blot analysis was performed using liver and kidney tissues from the index patient, as presented in Fig. 5B. The protein expression levels of the nuclear-encoded OXPHOS complex I protein NDUFA13 were decreased in the liver tissues; however, they were unchanged in the kidney tissues. The protein expression levels of SDHB and the core protein subunit, UQCRC2, from the OXPHOS complex III, were not changed in either the liver or the kidney, while ATP5A expression levels were decreased in both the liver and kidney tissues.

Discussion

The association between GFM1 gene defects and the recessively inherited mitochondrial disorder of oxidative phosphorylation was first reported 15 years ago (3). Over the past decade, the number of families identified to have mutations in this gene is only 25 (3-13). These patients demonstrated diverse phenotypes; however, the most prevalent clinical feature was liver disease, lactic acidosis, encephalopathy, feeding problems and failure to thrive (11). In the present study, a family with GFM1 mutations has been described; two siblings who were compound heterozygous for two missense mutations: C1576T, which, to the best of our knowledge; was reported for the first time; and G688A, which expands the range of GFM1 variants to 28.

In the literature (3-13), the majority of patients with GFM1 variants presented with fetal intrauterine growth retardation or developmental delay after birth. A variable neurological manifestation was identified from the beginning stage of life, including hypotonia, dystonia and feeding difficulties, as well as corresponding brain neuroimaging abnormalities. Liver involvement was considered to be an important diagnostic hallmark of GFM1-associated diseases; however, it has not been observed in an increasing number of recently reported patients with GFM1 mutations (4,5,8,12). The index patient in the present study developed the most common developmental, nervous and hepatic features, in concordance with previously reported cases (3-7,9-13). Notably, he also presented with structural alterations in the kidneys, with functional compensation, which has not been mentioned in previous case studies.

Apart from 2 cases (9,11), all the patients with GFM1 defects did not survive beyond infancy. In the present study, the index patient received a genetic diagnosis prior to birth and high-quality medical care in a university hospital and lived for >3 months, while his older sister only lived for 1 week, even though both siblings carried the same GFM1 mutations. The different ages of death in the two siblings was primarily due

to intrafamilial variability, which was consistent with previous reports (3,11). In addition, as the clinical and laboratorial data of the female sibling were not adequate, we hypothesized that the difference in severity between the two siblings was also partly due to timeliness and the level of medical care they received. Furthermore, preimplantation genetic diagnosis was recommended to the parents in the present study for their next pregnancy.

As a GTPase, the EFG1 protein catalyzes the delivery of peptidyl-tRNA from the ribosomal A site to the P site, following the formation of the peptide bond (6). EFG1 has been demonstrated to interact with both 50S large ribosomal subunit, near the L7/L12 stalk and the sarcin-ricin region of 23S rRNA (17). Only loss of both functional alleles could cause the mitochondrial translation defect in patients (13). EFG1 consists of 751 amino acids and includes 5 Pfam domains (10). The predictive data in the present study revealed that the two patients were heterozygous for a missense allele, which produces a conformational change in the GTP-binding domain I, and a non-sense allele, which has been predicted to cause an elimination of part of domain IV and the whole of domain V. The G688A mutation was reported by Balasubramaniam *et al* in 2012 (7); however, to the best of our knowledge, the C1576T mutation was identified for the first time in the present study (7). On one hand, the G230 substitution is located in the GTP EFTu domain I, a GTP binding domain, which is exposed to conformational changes mediated by the hydrolysis of GTP to GDP (10); on the other hand, the R526 premature stop codon is located in the EFG IV domain, which appears to be essential for the extensive structural rearrangement for tRNA-mRNA movement to occur, through extension similar to a lever arm (18). Therefore, we hypothesized that, if translated, it would generate a truncated polypeptide without a functional C-terminal block, as domains IV and V form the C-terminal block of EFG (18). In the present study, the pathogenicity of the novel mutation is theoretically supported by molecular modeling; the existence of the mutant GFM1 transcript associated with the c.1576C>T change was confirmed. The subsequent effects of the GFM1 protein on the expression levels of representative proteins in various OXPHOS complexes were further determined. The present study demonstrated that the levels of NDUFA13 were decreased in the liver; however, they were unchanged in the kidney. This observation was not surprising given that the nuclear-encoded OXPHOS complex I protein NDUFA13 is unstable during complex I assembly and is compromised in mitochondrial translation deficiencies (12), possibly in a tissue-specific manner. Consistent with previous observations (11), the expression level of the OXPHOS complex II protein SDHB was not attenuated in the present study, due to the exclusive nuclear genetic origin of the complex. The levels of UQCRC2, the core protein subunit from the OXPHOS complex III, were unaffected, as the only mtDNA polypeptide in complex III is cytochrome b (1). However, the ATP5A expression level was decreased in both the liver and kidney tissues in the index patient, while levels were reported to be stable in fibroblasts of a previous patient with a GFM1 mutation (12). Unfortunately, further research to clarify the activity of the OXPHOS complexes could not be conducted, as the samples of the index patient were not adequate.

In summary, the present study provided novel data for the mutational spectrum of GFM1 and additional patient phenotype information. Early genetic diagnosis and corresponding treatment would lead to an improved prognosis of this recessively inherited mitochondrial disorder.

Acknowledgements

Not applicable.

Funding

The present study was funded by the National Natural Science Foundation of China (grant no. 81873837 to FW), the Zhejiang Traditional Chinese Medicine Foundation (grant no. 2015ZQ025 to FW) and the Zhejiang Provincial Natural Science Foundation of China (grant no. LQ18H040005).

Availability of data and materials

The datasets used and/or analyzed during the present study are available from the corresponding author on reasonable request.

Authors' contributions

FW made substantial contributions to the conception and design of the study. CS performed the data acquisition, interpretation and analysis of the data. CS and FW were involved in data interpretation and drafting and revising the manuscript. FW gave final approval to the version to be published. All authors read and approved the final manuscript.

Ethics approval and consent to participate

Written informed consent and consent for publication to use samples and clinical data were obtained from the parents and the present study was formally approved by the Ethics Committee of The Women's Hospital, Zhejiang University School of Medicine, Zhejiang, China.

Patient consent for publication

Written consent for publication was obtained from all the parents.

Competing interests

The authors declare that they have no competing interests.

References

1. Wallace DC: A mitochondrial bioenergetic etiology of disease. J Clin Invest 123: 1405-1412, 2013.
2. Christian BE and Spremulli LL: Mechanism of protein biosynthesis in mammalian mitochondria. Biochim Biophys Acta 1819: 1035-1054, 2012.
3. Coenen MJ, Antonicka H, Ugalde C, Sasarman F, Rossi R, Heister JG, Newbold RF, Trijbels FJ, van den Heuvel LP, Shoubridge EA and Smeitink JA: Mutant mitochondrial elongation factor G1 and combined oxidative phosphorylation deficiency. N Engl J Med 351: 2080-2086, 2004.

4. Valente L, Tiranti V, Marsano RM, Malfatti E, Fernandez-Vizarra E, Donnini C, Mereghetti P, De Gioia L, Burlina A, Castellan C, *et al*: Infantile encephalopathy and defective mitochondrial DNA translation in patients with mutations of mitochondrial elongation factors EFG1 and EFTu. Am J Hum Genet 80: 44-58, 2007.
5. Smits P, Antonicka H, van Hasselt PM, Weraarpachai W, Haller W, Schreurs M, Venselaar H, Rodenburg RJ, Smeitink JA and van den Heuvel LP: Mutation in subdomain G' of mitochondrial elongation factor G1 is associated with combined OXPHOS deficiency in fibroblasts but not in muscle. Eur J Hum Genet 19: 275-279, 2011.
6. Antonicka H, Sasarman F, Kennaway NG and Shoubridge EA: The molecular basis for tissue specificity of the oxidative phosphorylation deficiencies in patients with mutations in the mitochondrial translation factor EFG1. Hum Mol Genet 15: 1835-1846, 2006.
7. Balasubramaniam S, Choy YS, Talib A, Norsiah MD, van den Heuvel LP and Rodenburg RJ: Infantile progressive hepatoencephalomyopathy with combined OXPHOS deficiency due to mutations in the mitochondrial translation elongation factor gene GFM1. JIMD Rep 5: 113-122, 2012.
8. Calvo SE, Compton AG, Hershman SG, Lim SC, Lieber DS, Tucker EJ, Laskowski A, Garone C, Liu S, Jaffe DB, *et al*: Molecular diagnosis of infantile mitochondrial disease with targeted next-generation sequencing. Sci Transl Med 4: 118ra110, 2012.
9. Brito S, Thompson K, Campistol J, Colomer J, Hardy SA, He L, Fernández-Marmiesse A, Palacios L, Jou C, Jiménez-Mallebrera C, *et al*: Corrigendum: Long-term survival in a child with severe encephalopathy, multiple respiratory chain deficiency and GFM1 mutations. Front Genet 6: 254, 2015.
10. Ravn K, Schonewolf-Greulich B, Hansen RM, Bohr AH, Duno M, Wibrand F and Ostergaard E: Neonatal mitochondrial hepatoencephalopathy caused by novel GFM1 mutations. Mol Genet Metab Rep 3: 5-10, 2015.
11. Simon MT, Ng BG, Friederich MW, Wang RY, Boyer M, Kircher M, Collard R, Buckingham KJ, Chang R, Shendure J, *et al*: Activation of a cryptic splice site in the mitochondrial elongation factor GFM1 causes combined OXPHOS deficiency. Mitochondrion 34: 84-90, 2017.
12. Barcia G, Rio M, Assouline Z, Zangarelli C, Gueguen N, Dumas VD, Marcorelles P, Schiff M, Slama A, Barth M, *et al*: Clinical, neuroimaging and biochemical findings in patients and patient fibroblasts expressing ten novel GFM1 mutations. Hum Mutat 41: 397-402, 2020.
13. Bravo-Alonso I, Navarrete R, Vega AI, Ruíz-Sala P, García Silva MT, Martín-Hernández E, Quijada-Fraile P, Belanger-Quintana A, Stanescu S, Bueno M, *et al*: Genes and variants underlying human congenital lactic acidosis-from genetics to personalized treatment. J Clin Med 8: 1811, 2019.
14. Wang X, Liu A, Lu Y and Hu Q: Novel compound heterozygous mutations in the *SPTA1* gene, causing hereditary spherocytosis in a neonate with Coombs-negative hemolytic jaundice. Mol Med Rep 19: 2801-2807, 2019.
15. Wang F, Pan J, Liu Y, Meng Q, Lv P, Qu F, Ding GL, Klausen C, Leung PC, Chan HC, *et al*: Alternative splicing of the androgen receptor in polycystic ovary syndrome. Proc Natl Acad Sci USA 112: 4743-4748, 2015.
16. Notredame C, Higgins DG and Heringa J: T-Coffee: A novel method for fast and accurate multiple sequence alignment. J Mol Biol 302: 205-217, 2000.
17. Sergiev PV, Bogdanov AA and Dontsova OA: How can elongation factors EF-G and EF-Tu discriminate the functional state of the ribosome using the same binding site? FEBS Lett 579: 5439-5442, 2005.
18. Salsi E, Farah E, Dann J and Ermolenko DN: Following movement of domain IV of elongation factor G during ribosomal translocation. Proc Natl Acad Sci USA 111: 15060-15065, 2014.